Dalton Transactions

Accepted Manuscript

ROYAL SOCIETY OF CHEMISTRY

www.rsc.org/dalton

Aerosol-assisted CVD of SnO from Stannous Alkoxide Precursors

Michael S. Hill,*[a] Andrew L. Johnson,*[a] John P. Lowe,[a] Kieran C. Molloy,[a] James D. Parish,[a] Thomas Wildsmith,[a] Andrew L Kingsley[b]

[a]*Department of Chemistry, University of Bath, Claverton Down, Bath, BA2 7AY, UK*

[b]*SAFC Hitech Ltd, Bromborough, Wirral, CH62 3QF, UK*

Abstract

*The stannous alkoxides [Sn(OR)$_2$] [R = i-Pr, t-Bu, C(Et)Me$_2$, CHPh$_2$, CPh$_3$] have been synthesised by reaction of Sn(NR'$_2$)$_2$ with two equivalents of HOR [R' = Me, R = i-Pr; R' = SiMe$_3$,R = t-Bu, C(Et)Me$_2$, CHPh$_2$, CPh$_3$]. Single crystal X-ray diffraction analysis of the bis(diphenylmethoxide) (**4**) and bis(triphenylmethoxide) (**5**) species have shown them to comprise three-coordinate Sn(II) centres through dimerisation in the solid state with the alkoxide units adopting transoid and cisoid configurations across the {Sn$_2$O$_2$} cores respectively. Thermogravimetric analysis indicates clean decomposition and some evidence of volatility at temperatures >200°C for all three aliphatic alkoxides, whereas both the diphenyl- and triphenylmethoxide compounds provide higher decomposition temperatures and, for the triphenylmethoxide derivative, a residual mass consistent with the formation of a carbon-containing residue. The previously reported iso-propoxide (**1**) and tert-butoxide (**2**) derivatives have been utilised in toluene solution to deposit SnO thin films by aerosol-assisted chemical vapour deposition (AACVD) on glass at temperatures between 300 and 450°C. While SnO is deposited under hot wall conditions as the only identifiable phase by p-XRD and Raman spectroscopy for both precursors, morphological analysis by SEM reveals inferior substrate coverage in comparison to previously reported ureide-based precursor systems.*

Introduction

Tin(II) alkoxides [Sn(OR)$_2$] have been known for several decades and are one of the key entry points to more elaborate derivatives of tin in its lower common oxidation state.[1] As such, this family of

compounds has been the subject of numerous synthetic and structural studies, while in more recent years their utility in the field of materials chemistry has come to the fore. In the solid state, when R is of low steric demands (e.g R = Me, Et[2]) the compounds display only limited solubility and, while they remain structurally uncharacterised, are unquestionably polymeric in nature. Although still polymeric, stannous alkoxides with larger R groups (e.g R = CH_2CMe_3, *i*-Pr)[3] display greater solubility, while more bulky organic substituents still lead to dimers (R = *t*-Bu [4,5], $C(2\text{-}C_4H_3S)_3$ [6]) or monomers (R = $C(t\text{-}Bu)_3$[7], various 2,6-substituted phenyl ligands[8-12]). Monomeric species can also be generated by the addition of suitable donor ligands e.g. $[Sn\{OCH(CF_3)_2\}_2.Me_2NH]$.[13]

From the perspective of materials chemistry, $Sn(OR)_2$ species provide intriguing precursors for tin oxide as, in principle, they could generate either SnO (by oxidation-state control) or SnO_2 (by precursor stoichiometry control). Indeed, previous deposition studies with tin(II) alkoxides have generated a variety of products depending on the constitution of the alkoxide ligand and the reaction conditions. Caulton and co-workers found that deposition using $[Sn(Oi\text{-}Pr)_2]$ (**1**) in low pressure CVD (LPCVD) experiments with no carrier gas resulted in the formation of tin metal at 295°C.[14] The volatile products from the deposition process were found to contain only acetone and HO^iPr suggesting that no cleavage of the C-O bond required for SnO_2 formation had occurred. Boyle *et al*. explored the use of $[Sn(OCH_2CMe_3)_2]_\infty$ as a LPCVD precursor for tin oxide.[15] Deposition was carried out on silicon wafers with the precursor vaporised at 130°C and with substrate temperatures between 315°C and 500°C to yield a mixed phase material of SnO, Sn_2O_3, SnO_2 and Sn^0. Although the relative ratios of the oxides were not determined, the authors did note that the tin metal content increased with temperature. A similar film composition was also obtained using the cage compounds $[Sn_5(O)_2(OCH_2CMe_3)_6]$ and $[Sn_6(O)_4(OCH_2CMe_3)_4]$, obtained by hydrolysis of $[Sn(OCH_2CMe_3)_2]$.[15,16] The deposition of mixed-phase films is consistent with the known thermal disproportionation of $[Sn(Ot\text{-}Bu)_2]$ (**2**) to Sn^0 and $[Sn(Ot\text{-}Bu)_4]$, generating core-shell SnO_2@Sn[17,18] and of SnO itself to Sn^0 + SnO_2 at temperatures >300°C.[19-21] The key feature to emerge from this collective research (and our recent work cited below) is the importance of deposition temperature and precursor identity in determining the final materials composition.[21,22]

Our interest in this general area stems for the growing importance of SnO as a *p*-type transparent conducting oxide (TCO), which complements the widely-exploited *n*-type SnO_2.[1,23] SnO is a wide bandgap semiconductor (2.7 - 3.4 eV) which has attracted interest as an anode material in rechargeable lithium-ion batteries,[24] but perhaps has greater promise as a component of all-tin oxide *p*-*n* heterojunctions.[25,26] Although CVD precursors for phase pure homogeneous SnO remain rare, we have recently reported the viability of species such as $[Sn(OSiMe_3)_2]$ (aerosol-assisted CVD; AACVD), $[Sn_6(O)_4(OSiMe_3)_4]$ (liquid-injection CVD, LICVD)[27] and the *bis*-ureide $[Sn\{N(Bu^t)C(O)NMe_2\}_2]$ (AACVD)[28] in this regard. We now report on the structural and materials chemistry of $Sn(OR)_2$ [R = *i*-Pr (**1**), *t*-Bu (**2**), $C(Et)Me_2$ (**3**), $CHPh_2$ (**4**), CPh_3 (**5**)] which complements and extends previous work in this area.

Results and Discussion

$[Sn(OR)_2]$ [R = *i*-Pr (**1**), *t*-Bu (**2**), $C(Et)Me_2$ (**3**), $CHPh_2$ (**4**), CPh_3 (**5**)] were synthesised by reaction of $Sn(NR'_2)_2$ with two equivalents of HOR [R' = Me, R = *i*-Pr; R' = $SiMe_3$, R = *t*-Bu, $C(Et)Me_2$, $CHPh_2$, CPh_3] (Eq. 1). The preparation of **1** and **2** has previously been achieved by protonolysis of $[Sn\{N(SiMe_3)_2\}_2]$ with *i*-PrOH and *t*-BuOH respectively.[3-5] Compounds **1**, **2**, **4** and **5** were isolated as colourless crystalline solids from toluene or hexane solutions, whereas compound **3** was isolated as an analytically pure pale yellow oil after removal of volatiles from the reaction.

$$Sn(NR'_2)_2 \xrightarrow{2\ ROH} [Sn(OR)_2]_n + 2HNR_2 \qquad (1)$$

R = Pr^i (**1**), CMe_3 (**2**), $C(Et)Me_2$ (**3**), $CHPh_2$ (**4**), CPh_3 (**5**)

The solid-state structure of compound **4** was deduced from a single crystal X-ray diffraction analysis (Table 1), the results of which are shown in Figure 1. Compound **4** adopts a centrosymmetric dimeric structure reminiscent of that previously deduced for $[Sn(Ot\text{-}Bu)_2]_2$ (**2**) with terminal and μ^2-bridging *tert*-butoxide ligands.[7] Like **5**, the $\{Sn_2O_2\}$ heterocycle is effectively planar with the organic residues oriented with a relative *transoid* disposition such that the steric interactions between the stereochemically active Sn(II) lone pairs are minimised.

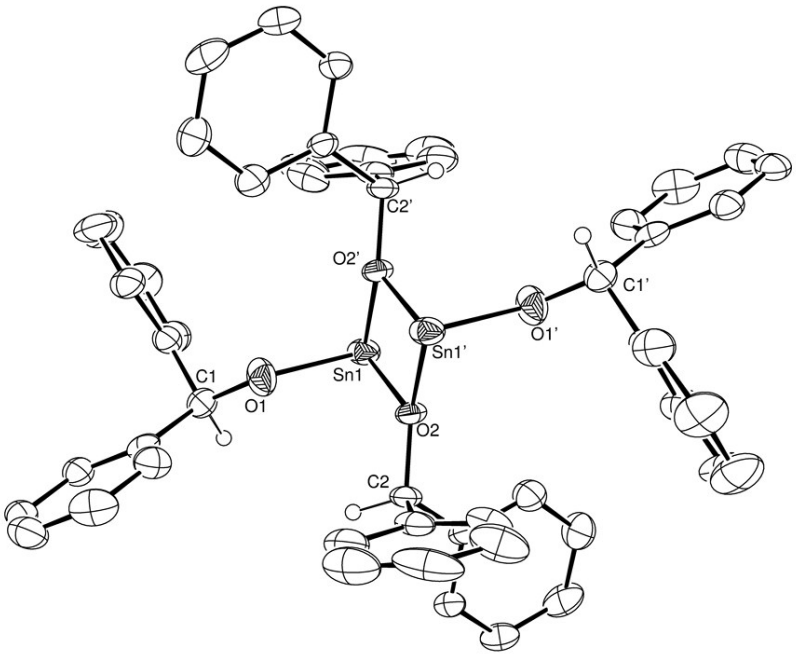

Figure 1: ORTEP representation of compound **4**. Thermal ellipsoids set at 25% probability. Hydrogen atoms, except those attached to C(1) and C(2) are removed for clarity. Selected bond lengths (Å) and angles (°): Sn(1)-O(1) 2.015(3), Sn(1)-O(2) 2.163(3), Sn(1)-O(2') 2.128(3), O(1)-C(1) 1.427(6), O(2)-C(2) 1.441(5), O(1)-Sn(1)-O(2) 84.95(14), O(1)-Sn(1)-O(2') 86.85(13), Sn(1)-O(2)-Sn(1') 107.95(12). Symmetry transformations used to generate equivalent atoms: ' -x+1,-y+2,-z+1.

Although the triphenylmethoxide derivative (**5**) is a similarly dimeric species (Figure 2), like the previously reported tris(2-thienyl)methoxide derivative,[6] the terminal alkoxide ligands of **5** adopt a *cisoid* orientation. Although this contrasting feature may simply reflect the differing relative steric demands of the alkoxide ligands, we tentatively suggest that the adoption of the *transoid* orientation in **5** may also be a consequence of the higher potential for stabilising dispersion interactions between the aromatic hydrocarbon substituents across the $\{Sn_2O_2\}$ ring.[29]

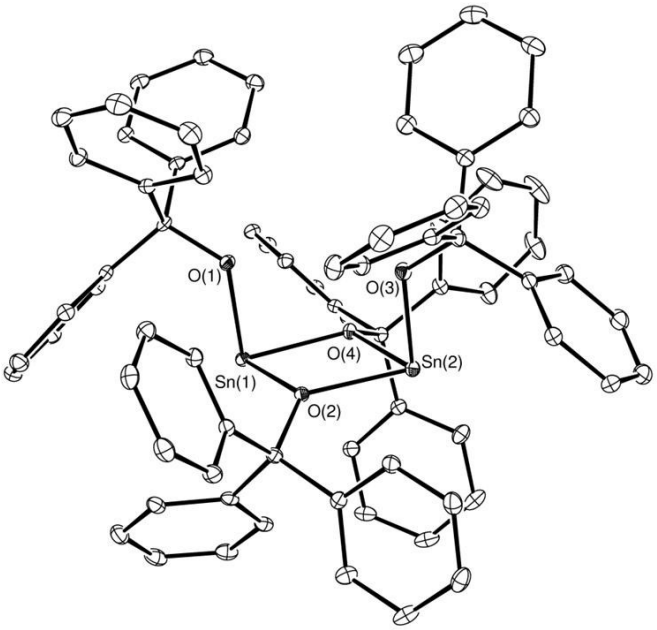

Figure 2: ORTEP representation of compound **5**. Thermal ellipsoids set at 40 % probability. Hydrogen atoms and THF molecules which co-crystallise have been removed for clarity. Selected bond lengths (Å) and angles (°): Sn(1)-O(1) 2.049(2), Sn(1)-O(2) 2.2324(19), Sn(1)-O(4) 2.1854(19), Sn(2)-O(2) 2.1890(19), Sn(2)-O(3) 2.045(2), Sn(2)-O(4) 2.2135(19), O(1)-C(1) 1.422(3), O(2)-C(2) 1.464(3), O(3)-C(3) 1.426(3), O(4)-C(4) 1.447(3), O(1)-Sn(1)-O(2) 90.02(8), O(1)-Sn(1)-O(4) 88.62(8), O(2)-Sn(1)-O(4) 73.76(7), O(2)-Sn(2)-O(3) 90.27(8), O(2)-Sn(2)-O(4) 74.07(7), O(3)-Sn(2)-O(4) 91.02(8), Sn(1)-O(4)-Sn(2) 106.43(8), Sn(1)-O(2)-Sn(2) 105.65(8).

Compounds **1** and **2** provided solution NMR data consistent with those reported previously.[3-5] Although a polymeric chain structure with doubly bridging isopropoxide ligands in the solid state, NMR diffusion measurements have shown that compound **1** exists predominantly as a dimer in toluene solution.[3b] The $^{119}Sn\{^{1}H\}$ chemical shift of compound **3** (δ –99.0 ppm) in d_8-toluene is comparable to that reported for $[Sn(O\textit{t}\text{-}Bu)_2]_2$ (**2**) (δ –93.6 ppm),[7] which has previously been assigned as maintaining a dimeric structure in solution. Although **4** and **5** were obtained as analytically pure crystalline solids and yielded ^{1}H and $^{13}C\{^{1}H\}$ NMR data which were consistent with the presence of single alkoxide ligand environments, the ^{119}Sn NMR spectra of both compounds in d_8-THF comprised two resonances (**4**, δ –181.1, –262.5 ppm: **5**, –243.7, –328.2 ppm). While the

intensity of the higher frequency signal of **4** was insignificant in comparison to its higher field partner, the resonances observed for compound **5** were of a comparable intensity. ^{119}Sn diffusion NMR (DOSY) experiments performed on the solution of compound **5** indicated that the molecules giving rise to both environments were diffusing at comparable rates and hence defined similar molecular radii. These data and the similarity of the ^{119}Sn chemical shifts to that reported for compound **1** (δ = –200.4 ppm) lead us to suggest that both compounds also display a similar dimeric constitution in THF solution.[3b] The ^{119}Sn{^{1}H} spectrum of compound **5** did not change on heating to 323 K, however, only the higher field resonance could be observed on lowering the temperature to 183 K. Although ^{119}Sn magnetisation transfer and EXSY experiments implied that the two environments were not undergoing chemical exchange, we suggest that these observations are an artefact of slow solution exchange between two isomeric forms of **5**, which cannot be discriminated as a result of the very rapid relaxation of the ^{119}Sn nucleus (T_1 = ca. 1×10^{-3} s). On this basis, we postulate that both compounds **4** and **5** adopt similar μ^2-alkoxo bridged dimeric structures in solution, both of which can exist as a pair of conformational isomers differentiated by a slow interchange between the *transoid* or *cisoid* disposition of the bridging substituents with respect to the {Sn_2O_2} plane. The potential for such isomerism is confirmed by the contrasting solid-state structures of the two compounds.

Thermogravimetric analysis (TGA) of compound **5** was indicative of negligible volatility and provided a residual mass (ca. 30.2%) significantly in excess of that expected for SnO (21.1%) or SnO_2 (23.6%). Although compound **4** provided a mass loss indicative of significant volatility (ca. 18.3%), the temperature required to effect a stable residue (>450 °C) was significantly in excess of that displayed by all three of the aliphatic alkoxide derivatives (**1** - **3**, Figure 3). The latter compounds exhibited similar thermal profiles and lost mass as a function of temperature at a similar rate. Compounds **1** and **3** displayed secondary mass loss events at around 20%, in both cases below the residual mass expected for tin metal. The ultimate residual masses for all three compounds are also similar, with **1** and **2** having nearly identical residues of 2.0 and 1.5% respectively. Although the

residual mass for compound **3** was slightly higher at 5.0%, these data indicate that all three compounds exhibit some volatility at elevated temperatures.

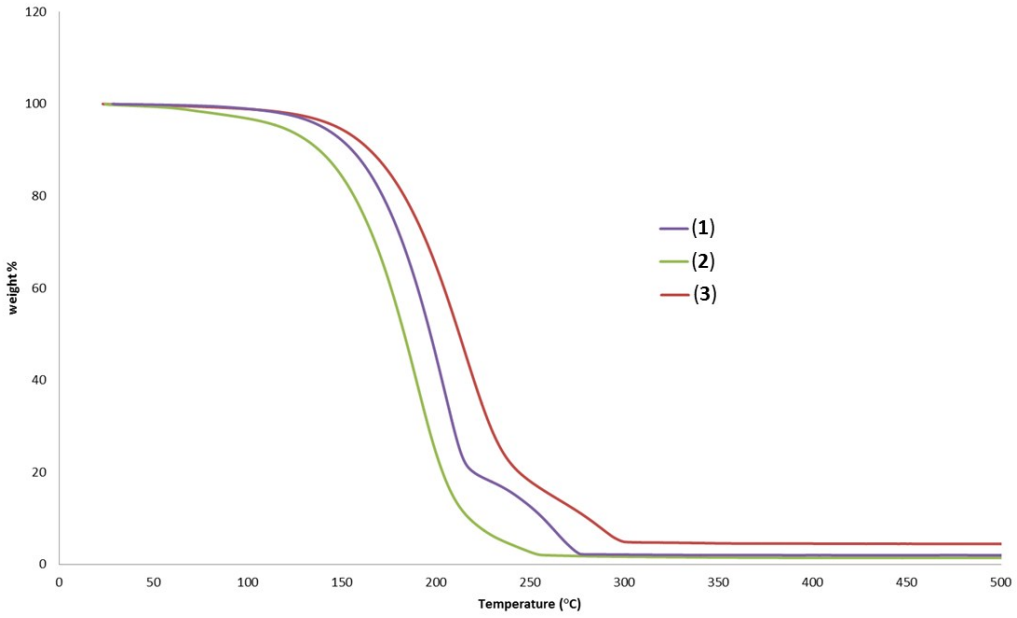

Figure 3: Comparison of TGA curves for compounds **1** - **3**.

Thin film deposition was carried out on silica-coated glass substrates (Pilkington-NSG) using the most readily handled stannous alkoxide derivatives, compounds **1** and **2**, under AACVD conditions using 0.03M solutions in toluene. The resultant films deposited using **1** at 250°C were adherent (Scotch tape test) and light brown in colour, while an increase of the deposition temperature to 300°C resulted in a stronger brown colouration at the expense of increased haze and a powdery composition. An increase of the deposition temperature to 350°C worsened the haze and increased the powdery nature of the film surface while further films prepared at 400°C were also hazy and powdery with some visibly metallic patches. The films were consequently deemed too inconsistent for meaningful optical or electrical analysis. Attempted deposition using a similar toluene solution of **2** showed no evidence of film growth at 300°C and only limited evidence of deposition at 350°C. Films grown at 400°C and 450°C, however, were visually much thicker and had a dark brown hue, with some sections looking metallic. The yellow-brown colour of these films were similar to that

observed for the films deposited using the tin(II) ureide, [Sn{(*t*-BuN)C(O)(NMe_2)}$_2$],[28] and would suggest that the films grown were predominately tin monoxide.

The EDS spectra of all these films contained signals corresponding to tin and oxygen as expected alongside additional peaks for silicon, magnesium and potassium, all components in glass. No carbon or nitrogen contamination could be detected in the deposited films within the detection limits of the instrument (<1%).

The powder X-ray diffraction (p-XRD) patterns of films grown using **1** at three different substrate temperatures are shown in Figure 4. The material grown shows crystalline phases at 300-400°C which correspond to SnO as the sole crystalline material present. These films show a greater degree of orientation than those deposited using **2** (*vide infra*) with the main diffraction lines corresponding to the (111), (200) and (112) planes. The substrate temperature does not seem to have a significant influence on the relative intensity of the diffraction peaks although the deposition carried out at 400°C provided the most intense diffraction maxima.

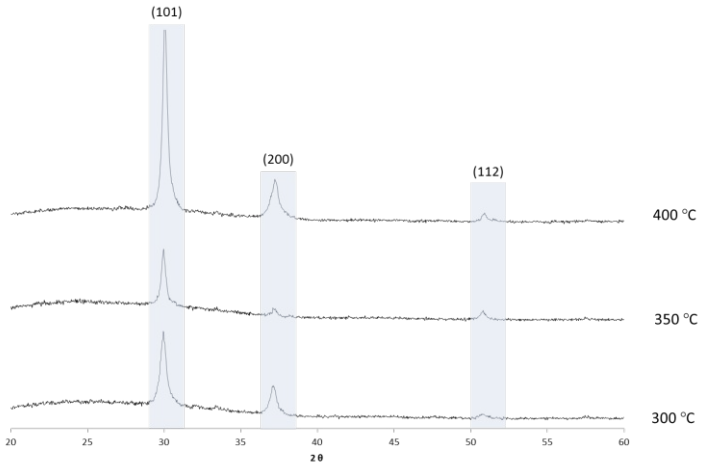

Figure 4: p-XRD patterns for samples grown on glass at varying deposition temperatures using precursor **1**.

The Raman spectrum for a sample grown on glass using **1** at 400°C is shown in Figure 5 and contains two vibrations (109, 209 cm^{-1}) corresponding to the B_{1g} and A_{1g} modes observed in SnO.[30] This endorses the single-phase SnO deposition evident in the p-XRD analysis. Although the

deposition at 250°C provided no Raman active vibrations, the yellow colouration suggested some film growth which could be too thin to be detectable by vibrational spectroscopy. Thin films deposited at 300°C and 350°C, however, provided Raman spectra comparable to that shown in Figure 5 with limited change in intensity of the observed vibrations.

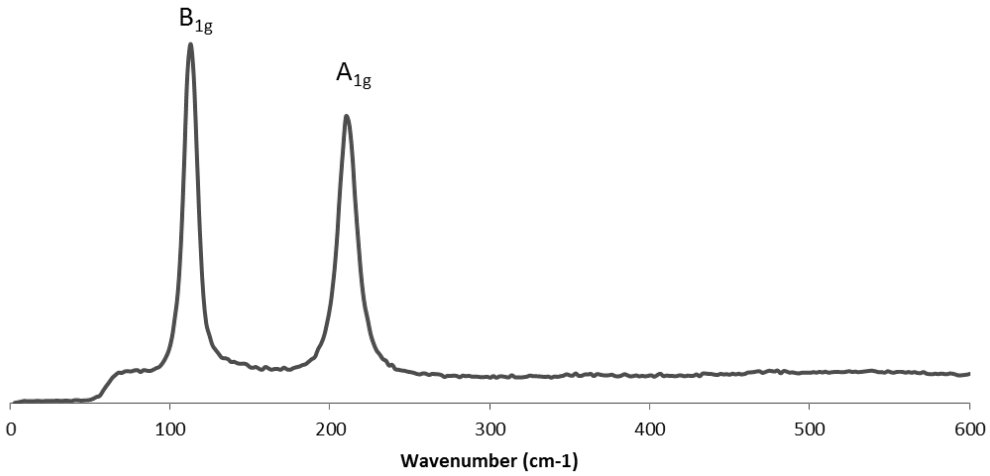

Figure 5: Raman spectrum of SnO sample grown at 400°C on glass using compound **1**.

p-XRD analysis of films grown at different substrate temperatures using compound **2** are shown in Figure 6. The materials grown comprise crystalline phases at substrate temperatures in excess of 400°C, with the diffraction maxima assigned to tetragonal SnO (*P*4/*mmm*). Notably, the p-XRD patterns show no evidence of crystalline SnO_2 or tin metal present in the films and have a random orientation. While the deposition carried out at 350°C provided no diffraction maxima, the Raman spectrum of the film deposited at this temperature displayed diagnostic B_{1g} and A_{1g} modes (109, 219 cm^{-1}) corresponding to SnO growth. A similar analysis of the substrate after attempted deposition at 300°C, however, displayed no Raman active modes, consistent with the observation of no visual film growth at this temperature.

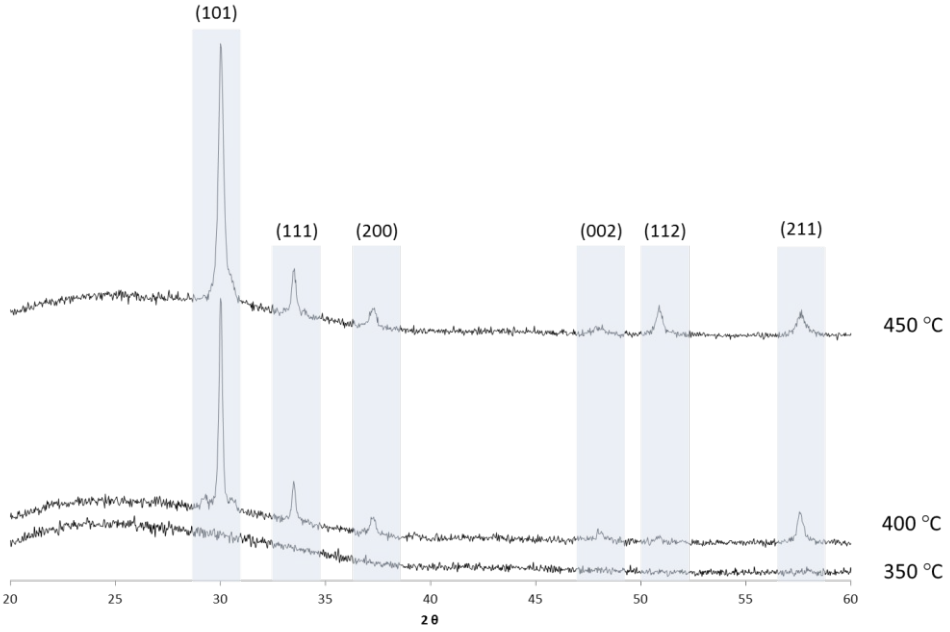

Figure 6: p-XRD patterns for samples grown on glass at varying deposition temperatures using compound **2**.

Figure 7a/b illustrates scanning electron micrographs of the surfaces of a typical SnO film deposited using **1** at 350°C. The low magnification image shows an apparently uniform film covered with a secondary material that has a different morphology (Figure 7a) while the high magnification (Figure 7b) reveals that the islands of material comprise of smaller spherical particles which are approximately 20-30 nm in diameter. These observations are most likely indicative of a mixture of both surface-mediated film growth and gas phase particulate nucleation and diffusion to the substrate surface. Notably, the crystallite size for films grown using **1** at 350°C derived from the XRD traces (101 reflection) using the Scherrer equation[31] ranged from 22 nm to 31 nm. The surface of the film deposited at 400°C using **2** was found to be discontinuous (Figure 7c). The material deposited has a unique morphology comprising 1-3 μm long cuboids (Figure 7d), each of which were observed to be made up of 100 nm spherical particles, giving the overall appearance of nano-"rice krispy cakes". Although these results indicate that both compounds **1** and **2** provide viable levels of Sn(II) oxidation state control for the formation of SnO, in neither case was the coverage and conformality of the resultant films comparable to those resulting from our earlier use of the bis-ureide derivative, [Sn{(*t*-

Bu)C(O)(NMe_2)$_2$}$_2$].[28] In this latter case the films were found to consist of uniform tightly packed platelets, more typical of SnO films deposited by physical and evaporative techniques.[32]

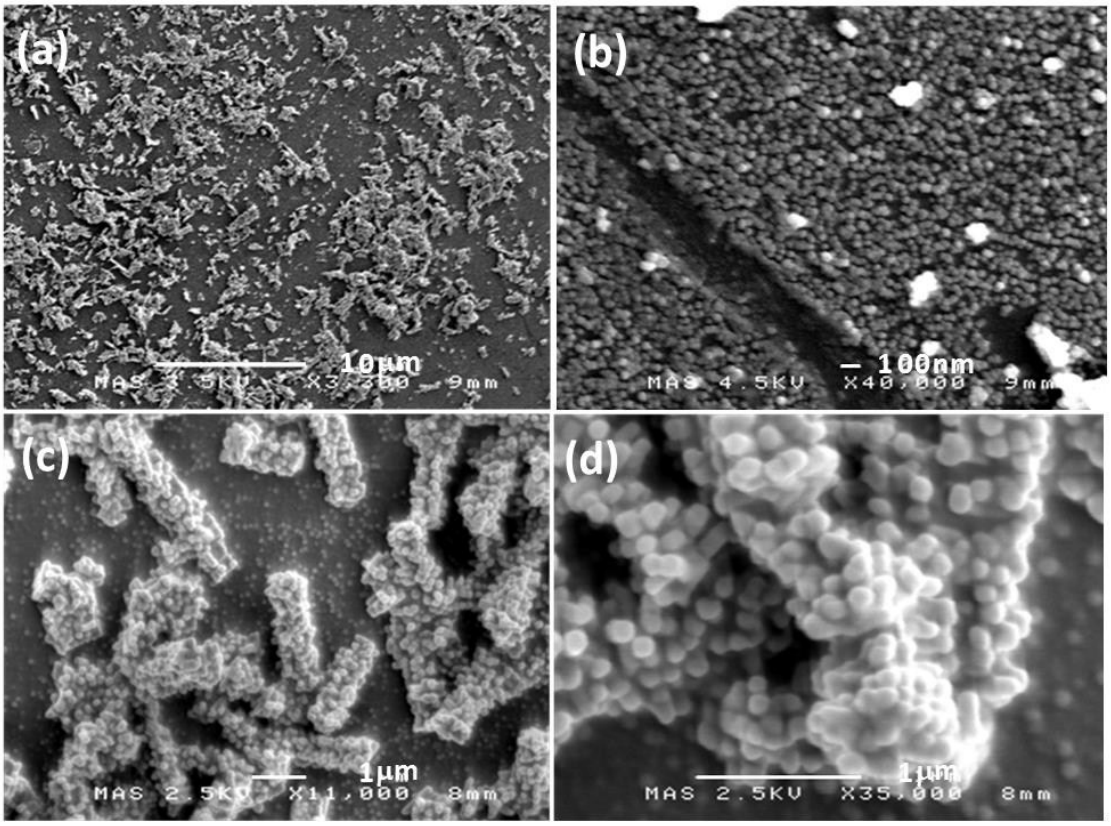

Figure 7: SEM micrographs of SnO grown at 350°C on glass using compound **1** at (a) 3,300 × and (b) 40,000 × magnification; SEM micrographs of SnO grown at 400°C on glass using compound **2** at (c) 11,000 × and (d) 35.000 × magnification.

Conclusions

Aerosol-assisted CVD using the tin(II) alkoxide compounds **1** and **2** resulted in the exclusive growth of SnO thin films on glass substrates. The deposition temperature was found to be affected by the identity of the precursor, with **1** showing growth at temperatures above 300°C while growth from **2** required temperatures exceeding 350°C. The morphology of the deposited films was found to vary depending on the precursor. While deposition carried out using **2** resulted in the formation of micron-sized cuboid particles comprised of smaller (*ca*. 100 nm) spherical units, thin films deposited using **1**

comprised smaller (<30 nm) particles but were found to be discontinuous and inferior to the films produced by our previously described bis-ureide precursor system.[28]

Experimental

All reactions were carried out under an argon atmosphere using standard Schlenk line and glovebox techniques in an MBraun Labmaster glovebox at O_2, H_2O < 2.5 ppm. NMR experiments using air-sensitive compounds were conducted in J. Youngs tap NMR tubes prepared and sealed in a glovebox under argon. NMR spectra were recorded either on a Bruker AV-400 spectrometer at 100.6 MHz (^{13}C) and 149.2 MHz (^{119}Sn), a Bruker AV-300 at 75.5 MHz (^{13}C), spectrometer or a Bruker AV-250 spectrometer at 62.9 MHz (^{13}C). The ^{1}H and ^{13}C NMR spectra were referenced relative to residual solvent resonances while the ^{119}Sn NMR spectra were referenced relative to an external standard (Me_4Sn). Unless otherwise stated data quoted were recorded at 298 K. Elemental analysis was performed by Mr. Stephen Boyer at SACS, London Metropolitan University. Solvents for air- and moisture-sensitive reactions were provided by an Innovative Technology Solvent Purification System, or dried/degassed manually according to established laboratory procedures. $[Sn(NMe_2)_2]_2$, $[Sn\{N(SiMe_3)_2\}_2]_2$, $[Sn(OPr\text{-}i)_2]$ (**1**) and $[Sn(OBu\text{-}t)_2]_2$ (**2**) were prepared by literature methods.[33-35, 3,4,5]

TGA analysis of the complexes was performed at SAFC Hitech, Bromborough, UK, using a Shimadzu TGA-51 Thermogravimetric Analyser. Data points were collected every second at a ramp rate of 20 °C min^{-1} in a flowing (50 ml min−1) N_2 stream. FE-SEM analysis of the films was undertaken on a JEOL 6301F. EDX analysis was performed using a JEOL 6480 LV SEM microscope. Powder XRD of the films was performed on a Bruker D8 Advance powder diffractometer, using a Cu anode X-ray source (Kα wavelength = 1.5406 Å) at the University of Bath.

Synthesis

Compound 3: A solution of $[Sn\{N(SiMe_3)_2\}_2]_2$ (3.1 g, 3.5 mmol) in THF (20 mL) was added to 2-methyl-2-butanol (1.2 g, 14 mmol) and left to stir for 20min. The solvent was removed *in vacuo* to

provide compound **3** as pale yellow oil in effective stoichiometric yield. Analysis, found [calc. for $C_{11}H_{24}SnO_2$] C 42.90 (43.03)%, H 7.56 (7.88)%. ^{1}H NMR (300 MHz, d_8-tol); δ 0.99-1.04 (t, 3H, CH_2CH_3, ^{3}J = 7.5Hz), 1.36 (s, 6H, $C(CH_3)_2$, 1.57-1.68 (quartet, 2H, CH_2CH_3, ^{3}J = 7.5 Hz). ^{13}C{^{1}H} NMR (75.5 MHz, d_8-tol); δ 28.6, 31.8, 33.8, 73.2. ^{119}Sn{^{1}H} NMR (111.8 MHz, d_8-tol); δ –99.0.

Compound 4: A solution of $[Sn\{N(SiMe_3)_2\}_2]_2$ (1.76 g, 4 mmol) in tolune (20 mL) was added to a solution of diphenyl methanol (1.47 g, 8 mmol) in toluene (20 mL) and stirred for 3 hours. The solution was filtered through Celite® and the volume reduced to afford colourless crystals of compound **2** at -28 ^{o}C. (0.86g, 44%). Analysis, found [calc. for $C_{26}H_{22}O_2Sn$]: C 64.28 (64.37)%, H 4.63 (4.57)%. ^{1}H NMR (300 MHz, d_8-THF); δ 6.09 (s, 2H, C*H*), δ 7.10-7.26 (br m, 12H, CH_{Ar}), δ 7.31-7.45 (br m, 8H, CH_{Ar}). ^{13}C NMR (75.5 MHz, d_8-THF); δ 78.76 (s, 2C, *C*H), δ 128.03 (br s, 16C, *o*/*m*-CH_{Ar}), δ 129.33 (s, 4C, *p*-CH_{Ar}), δ 147.52 (br s, 4C, *ipso*-C_{Ar}); ^{119}Sn NMR (111.8 MHz, d_8-THF); δ –181.1 (minor), –262.5 (major).

Compound 5: A solution of $[Sn\{N(SiMe_3)_2\}_2]_2$ (1.76 g, 4 mmol) in THF (20 mL) was added to a solution of triphenyl methanol (2.08 g, 8 mmol) in THF (20mL) and stirred for 3h. The solution was filtered through Celite® and the volume reduced to afford colourless crystals of compound **3** at –28^o C. (2.18g, 86%). Analysis, found [calc. for $C_{38}H_{30}O_2Sn$]: C 71.75 (71.61)%, H 4.82 (4.74)%. ^{1}H NMR (300 MHz, d_8-THF); δ 7.0-7.4 (m, 30H, C_6H_5). ^{13}C NMR (75.5 MHz, d_8-THF); δ 127.6, 128.8, 148.1 (C_6H_5). ^{119}Sn NMR (111.8 MHz, d_8-THF); δ -243.71, -328.19. Slow crystallisation from THF yielded crystals suitable for X-ray diffraction studies which contained one molecule of solvent.

Single Crystal X-ray Crystallography

Data for compound **4** (CCDC 1508117) were collected on a Xcalibur E X-ray Diffraction System while data for **5** (CCDC 1487174) were collected on a Nonius Kappa CCD diffractometer at 150(2) K using Mo-Kα radiation (λ = 0.71073 Å). Structure solution and refinement was performed using SHELX86[36] and SHELX97[37] software, respectively. Data were processed using the Nonius Software.[38] Structure solution,[39] followed by full-matrix least squares refinement was performed

using the WINGX-1.80 suite of programs throughout.[40] Hydrogen atoms were included at calculated positions. Details are given in Table 1.

Table 1: Crystallographic data for compounds **4** and **5**.

	4	**5**
Molecular formula	$C_{52}H_{44}O_4Sn_2$	$C_{84}H_{76}O_4Sn_2$
Formula weight (g mol^{-1})	970.25	1418.83
Crystal system	triclinic	monoclinic
Space group	P -1	$P\ 2_1/c$
a (Å)	9.7376(7)	12.49000(10)
b (Å)	10.0924(6)	13.0510(2)
c (Å)	12.1457(9)	40.6560(5)
α (deg)	77.187(6)	90
β (deg)	68.707(7)	92.1630(10)
γ (deg)	87.128(6)	90
V (Å^3)	1083.84(14)	6622.49(14)
Z	1	4
μ (mm^{-1})	1.197	0.811
ρ (g cm^{-3})	1.487	1.423
θ range (^{o})	3.384 to 27.507	2.95 to 27.51
R_1,[a] wR_2 [I > 2σ(I)][b]	0.0512, 0.1206	0.0403, 0.0743
R_1,[a] wR_2 (all data)[b]	0.0676, 0.1317	0.0626, 0.0808
Measured/independent reflections/ R_{int}	8636/ 4970/ 0.0283	88285/ 15167/ 0.0721

[a] $R1=\Sigma\ ||F_o|-|F_c||/\Sigma|F_o|$; [b] $wR_2=\{\Sigma[w(F_o^2-F_c^2)^2]/\Sigma[w(F_o^2)^2]\}^{1/2}$

Materials Chemistry

Thin films were deposited using a hot wall system comprised of a TSI 3076 Constant Output Atomiser using argon at 20 psi to generate the aerosol and act as carrier gas. The aerosol was passed through a quartz tube containing the glass substrate, heated by an Elite thermal Systems Ltd tube furnace. Details are given in Table 2.

Table 2: AACVD deposition details.

Precursor	**1**	**2**
Precursor concentration	0.03M toluene	0.03M toluene

Substrate temperature	250-400 °C	300-450 °C
Carrier gas flow rate	3.0 L/min	3.0 L/min
Deposition time	30 minutes	30-60 minutes

Acknowledgements

We thank the EPSRC (UK) for funding through the EPSRC Doctoral Training Centre in Sustainable Chemical Technologies (Grant No. EP/G03768X/1).

References

1. Tin Chemistry: Fundamentals, Frontiers, and Applications, Ed, A. G. Davies, K. Pannell, E. R. T. Tiekink, Wiley, 2008.
2. E. Amberger and M. R. Kula, *Angew. Chemie*, 1963, **75**, 476.
3. (a) T. J. Boyle, T. M. Alam, M. A. Rodriguez and C. A. Zechmann, *Inorg. Chem.*, 2002, **41**, 2574; (b) L. Wang, M. Bochmann, R. D. Cannon, J.-F. Carpentier, T. Roisnel and Y. Sarazin, *Eur. J. Inorg. Chem.*, 2013, 5896.
4. M. Veith and F. Toellner, *J. Organomet. Chem.*, 1983, **246**, 219.
5. (a) M. Veith, P. Hobein and R. Roesler, *Z. Naturforsch. B*, 1989, **44**, 1067; see also (b) L. Wang, C. E. Kefalidis, T. Roisnel, S. Sinbandhit, L. Maron, J.-F. Carpentier, and Y. Sarazin, *Organometallics*, 2015, **34**, 2139.
6. M. Veith, C. Belot, V. Huch and M. Zimmer, *Z. Anorg. Allg. Chem.*, 2009, **635**, 942.
7. T. Fjeldberg, P. B. Hitchcock, M. F. Lappert, S. J. Smith and A. J. Thorne, *J. Chem. Soc. Chem. Commun.*, 1985, **2**, 939.
8. B. Cetinkaya and I. Gumrukcu, *J. Am. Chem. Soc.*, 1980, **102**, 2088.
9. C. Stanciu, A. F. Richards, M. Stender, M. M. Olmstead and P. P. Power, *Polyhedron*, 2006, **25**, 477.
10. D. A. Dickie, I. S. MacIntosh, D. D. Ino, Q. He, O. A. Labeodan, M. C. Jennings, G. Schatte, C. J. Walsby and J. A. C. Clyburne, *Can. J. Chem.*, 2008, **86**, 20.
11. T. J. Boyle, T. Q. Doan, L. A. M. Steele, C. Apblett, S. M. Hoppe, K. Hawthorne, R. M. Kalinich and W. M. Sigmund, *Dalton. Trans.*, 2012, **41**, 9349.

12. D. M. Barnhart, D. L. Clark and J. G. Watkin, *Acta Crystallogr. Sect. C Cryst. Struct. Commun.*, 1994, **50**, 702.

13. S. Suh and D. Hoffman, *Inorg. Chem.*, 1996, **35**, 6164.

14. D. J. Teff, C. D. Minear, D. V. Baxter and K. G. Caulton, *Inorg. Chem.*, 1998, **37**, 2547.

15. T. J. Boyle, T. L. Ward, S. M. De'Angeli, H. Xu and W. F. Hammetter, *Chem. Mater.*, 2003, **15**, 765.

16. T. J. Boyle, T. M. Alam, M. A. Rodriguez and C. A. Zechmann, *Inorg. Chem.*, 2002, **41**, 2574.

17. M. Veith, S. Kneip, S. Faber and E. Fritscher, *Mater. Sci. Forum*, 1998, **269-272**, 303.

18. M. Veith, S. J. Kneip, A. Jungmann and S. Hufner, *Z. Anorg. Allg. Chem.*, 1997, **623**, 1507

19. H. Giefers, F. Porsch and G. Wortmann, *Solid State Ionics*, 2005, **176**, 199.

20. F. Gauzzi, B. Verdini, A. Maddalena and G. Principi, *Inorg. Chim. Acta*, 1985, **104**, 1

21. M. S. Moreno, G. Punte, G. Rigotti, R. C. Mercader, A. D. Weisz, B. M. A, *Solid State Ionics* 2001, **144**, 81.

22. Z. P. Titova, E. V. Savina and D. N. Klushin, *J. Appl. Chem. USSR* 1964, **37**, 2129.

23. K.C. Molloy, *J. Chem. Res.*, **2008**, 549.

24. D. Aurbach, A. Nimberger, B. Markovsky, E. Sominski and A. Gedanken, *Chem. Mater.*, 2002, **14**, 4155.

25. (a) R. G. Gordon, *MRS Bulletin*, 2000, **25**, 52; (b) Z. Wang, P. K. Nayak, J. A. Caraveo-Frescas and H. N. Alshareef, *Adv. Mater.*, 2016, **28**, 3831.

26. A. N. Banerjee and K. K. Chattopadhyay, *Prog. Cryst. Growth Charac. Mater.*, 2005, **50**, 52.

27. I. Barbul, A. L. Johnson, G. Kociok-Köhn, K. C. Molloy, C. Silvestru and A. L. Sudlow, *Chempluschem*, 2013, **78**, 866.

28. T. Wildsmith, M. S. Hill, A. L. Johnson, A. J. Kingsley and K. C. Molloy, *Chem. Commun.*, 2013, **49**, 8773.

29. J.-D. Guo, D. J. Liptrot, S. Nagase, and P. P. Power, *Chem. Sci.*, 2015, **6**, 6235.

30. L. Sangaletti, L. E. Depero, B. Allieri, F. Pioselli, E. Comini, G. Sberveglieri and M. Zocchi, *J. Mater. Res.*, 1998, **13**, 2457.

31. P. Scherrer, *Nachr. Ges. Wiss. Göttingen*, 1918, **26**, 98.

32. See, for example; (a) W. Guo, L. Fu, Y. Zhang, K. Zhang, L. Y. Liang, Z. M. Liu, H. T. Cao and Q. X. Pan, *Appl. Phys. Lett.*, 2010, **96**, 042113; (b) Y. Ogo, H. Hiramatsu, K. Nomura, H. Yanagi, T. Kamiya, M. Kimura, M. Hirano and H. Hosono, *Phys. Status Solid A*, 2009, **206**, 2187; (c) T. Toyama, Y. Seo, T. Konishi, H. Okamoto and Y. Tsutumi, *Appl. Phys. Express*, 2011, 071101; (d) P.-C. Hsu, W.-C. Chen, Y.-T. Tsai, Y.-C. Kung, C.-H. Chang, C.-J. Hsu, C.-C. Wu and H.-H. Hsieh, *Jpn. J. Appl. Phys.*, 2013, **52**, 05DC0; (e) K. C. Sanal and M. K. Jayaraj, *Mater. Sci. & Eng. B, Adv. Sol. State Mat.* 2013 **178**, 816.

33. P. Foley and M. Zeldin, *Inorg. Chem.*, 1975, **14**, 2264.

34. M. M. Olmstead and P. P. Power, *Inorg. Chem.*, 1984, **2**, 413.

35. H. Harris and M. F. Lappert, *J. Chem. Soc.*, 1974, 895–896.

36. G. M. Sheldrick, SHELX-86, Computer Program for Crystal Structure Determination, University Of Göttingen, Germany, 1986.

37. (a) G. M. Sheldrick, SHELX-97, Computer Program for Crystal Structure Refinement, University of Göttingen, Germany, 1997; (b) G. M. Sheldrick, *Acta Crystallogr., Sect. A: Fundam. Crystallogr*., 2008, **64**, 112.

38. Z. Otwinowski and W. Minor, *Methods Enzymol.*, 1997, **276**, 307.

39. A. Altomare, M. C. Burla, M. Camalli, G. L. Cascarano, C. Giacovazzo, A. Guagliardi, A. G. Moliterni, G. Polidori and R. Spagna, *J. Appl. Crystallogr.*, 1999, **32**, 115.

40. L. J. Farrugia, *J. Appl. Crystallogr.*, 2012, **45**, 849.

For Table of Contents use: